Talanta 114 (2013) 254–260

Contents lists available at SciVerse ScienceDirect

Talanta

journal homepage: www.elsevier.com/locate/talanta

Resolution of lysosomes in living cells with a ratiometric molecular pH-meter

Zhu Li [a,1], Shuqi Wu [a,1], Jiahuai Han [b], Liu Yang [a,*], Shoufa Han [a,**]

[a] Department of Chemical Biology, College of Chemistry and Chemical Engineering, and the Key Laboratory for Chemical Biology of Fujian Province, PR China
[b] The Key Laboratory of the Ministry of Education for Cell Biology and Tumor Cell Engineering, School of Life Science College of Life Science, Xiamen University, Xiamen, PR China

ARTICLE INFO

Article history:
Received 12 March 2013
Received in revised form
10 May 2013
Accepted 19 May 2013
Available online 6 June 2013

Keywords:
Ratiometric imaging
Molecular pH-meter
Apoptosis
Lysosomal acidity

ABSTRACT

Intracellular acidic vesicles, constituted mostly by lysosomes, mediated a variety of biological events ranging from endocytosis, apoptosis, to cancer metastasis, etc. A chimeric molecular pH-meter (Lyso-DR), comprised of a dansyl fluorophore and proton activatable rhodamine-lactam, was prepared for ratiometric reporting of intralysosomal acidity. Exclusively confined in lysosomes, Lyso-DR exhibited pH dependent dual fluorescence emission bands which enable resolution of individual lysosomes in terms of acidity and quantitation of the overall intracellular lysosomal acidity, e.g. the lysosomal pH of HeLa cells is around pH 5.0 whereas that of L929 cells is around pH 6.2. Lyso-DR effectively differentiated the lysosomal pH changes of cells undergoing apoptosis vs necrosis, suggesting its utility in investigations on lysosome involved biomedical processes.

1. Introduction

pH homeostasis inside eukaryotic cells is maintained in an organelle-dependant manner. Intracellular acidic compartments, including lysosomes, endosomes, and autophagosome, etc., are dynamically dispersed in cytoplasma which is slightly alkaline at about pH 7.2. The acidity of these acidic vesciles (mostly lysosomes) is crucial for endocytosis, and autophagy, etc. Aberrant alterations of the intracompartmental pH have been implicated in a number of biological events, such as cancer development, cell differentiation and cell death [1–3]. Cell death normally occurs by two alternative, opposite modes: apoptosis, a programmed form of cell death, and necrosis, an unordered and accidental form of cellular death [4]. Lysosomes have received considerable attention in the pathogenesis of cell apoptosis [5,6] and necrosis [7]. Noninvasive methods that enable accurate mapping of the dynamic changes of lysosomal pH in living cells would be valuable for investigations on the impacts of lysosomal acidity on apoptosis and necrosis.

Among dyes widely used for intracellular pH studies [8], fluorescein derivatives are less emissive in lysosomal environments due to protonation of the phenolate moiety which is critical for optimal fluorescence emission. Commercial LysoTrackers, exhibiting enhanced fluorescene at acidic pH, is limited by liability to photo bleaching and relative high background signals. Despite recent advances in ratiometric pH probes that could overcome the uncertainties associated with single intensity based fluorophores [9–14], ratiometric bioimaging of the acidity of individual lysosomes have been largely unexplored. Given the challenges in design of single fluorophore based probes with pH dependant dual emission bands, we report the integration of two widely used fluorophores, proton activatable rhodamine-lactam and dansyl moiety, which gives a self-referenced lysotrophic molecular pH-meter enabling ratiometric reporting of lysosomal acidity in living cells.

2. Experimental

2.1. Materials and methods

LysoSensor Yellow/Blue and LysoTracker Green DND-26 were purchased from Invitrogen. All other chemicals were obtained from Alfa Aesar unless specified. NMR spectra (^{1}H at 400 MHz and ^{13}C at 100 MHz) were recorded on a Bruker instrument using tetramethylsilane as the internal reference. Mass analysis was performed in Bruker En Apex ultra 7.0T FT-MS. Fluorescence and UV–vis spectra were recorded on a spectrofluorometer (SpectraMax M5, Molecular Device). L929 cells and HeLa cells were obtained from American Type Culture Collection (ATCC). Confocal

* Corresponding author. Tel.: +86 0592 2181728.
** Corresponding author.
E-mail addresses: yangliu@xmu.edu.cn (L. Yang), shoufa@xmu.edu.cn (S. Han)
[1] Both authors contribute equally to this work.

0039-9140/$ - see front matter © 2013 Elsevier B.V. All rights reserved.
http://dx.doi.org/10.1016/j.talanta.2013.05.036

fluorescence microscopy images were obtained on Zeiss780 using the following filters: λ_{ex}@488 nm and λ_{em}@500–520 nm for LysoTracker Green DND-26 signal; λ_{ex}@543 nm and λ_{em}@565–625 nm for rhodamine 6G-amide signal; λ_{ex}@405 nm and λ_{em}@410–470 nm for dansyl signal. The fluorescence of LysoTracker Green DND-26 and that of Lyso-DR inside cells were merged by using Photoshop CS 5.0. For ratiometric analysis, the fluorescence emission of dansyl fluorescence was recorded with filter FL1 (410–470 nm) while that of R6G-amide was recorded by filter FL2 (565–625 nm). 10,000 cells were analyzed and the data were processed by Origin 8.5. Detailed procedures for the synthesis of R6G-lactam-diethylenetriaminde, Dansyl-EDA-R6G and Lyso-DR can be found in Supporting information (S1–S3).

2.2. Ratiometric pH titration of Lyso-DR and Dansyl-R6G under dual wavelength excitation

An aliquot of Lyso-DR stock or Dansyl-EDA-R6G solution (1 mg/mL) in DMF was respectively added to sodium phosphate buffers (200 mM) of various pHs to a final concentration of 10 μg/mL. The fluorescence emission spectra were recorded as a function of pH using λ_{ex}@300 nm for dansyl fluorescence emission and λ_{ex}@530 nm for R6G-lactam.

2.3. Ratiometric pH titration of Lyso-DR under single wavelength excitation

Aliquots of Lyso-DR stock solution in DMF were added to sodium phosphate buffers of various pH values to a final concentration of 1 μg/mL. The fluorescence emission spectra were recorded as a function of pH using λ_{ex}@300 nm.

2.4. Staining of lysosomes with Lyso-DR in living cells

L929 cells were seeded on 35 mm glass-bottom dishes (NEST) and incubated in DMEM medium for 24 h, followed by addition of LysoTracker Green (40 ng/mL) and Lyso-DR (1 μg/mL). The cells were further incubated in fresh DMEM medium for 30 min and then analyzed with a confocal fluorescence microscope. The blue emissions (dansyl) in 410–470 nm was collected using an excitation wavelength of 405 nm; the red emissions (R6G-amide) in 550–630 nm was collected using an excitation wavelength of 543 nm while the green emissions (LysoTracker Green) in 490–525 nm was collected using an excitation wavelength of 488 nm. Images were merged with Photoshop CS 5.0.

2.5. pH dependent staining of lysosomes with Lyso-DR

L929 cells and HeLa cells were respectively incubated in DMEM medium spiked with or without 100 nM of bafilomycin A1 (BFA) for 4 h. Cells were further cultured in DMEM medium containing Lyso-DR (1 μg/mL) for 30 min and then analyzed with a confocal fluorescence microscope. The blue emissions (dansyl) in 410–470 nm were collected using an excitation wavelength of 405 nm; the red emissions (R6G-amide) in 550–630 nm were collected using an excitation wavelength of 543 nm.

2.6. pH titration with Lyso-DR in living cells

HeLa cells were seeded on 35 mm glass-bottom dishes and incubated in DMEM medium supplemented with Lyso-DR (1 μg/mL) for 24 h. The cells were further incubated in Briton buffer of various pHs supplemented with H^+/K^+ ionophore nigericin (100 nM) for 4 h, and then were analyzed by confocal fluorescence microscopy. The fluorescence emission of dansyl moiety at 410–470 nm was collected while the emission at 550–630 nm was collected for R6G-amide. The ratios were calculated by ImageJ software.

2.7. Staining of lysosomes with dansyl-EDA-R6G in living cells

L929 cells were seeded on 35 mm glass-bottom dishes and incubated in DMEM medium for 24 h, followed by addition of LysoTracker Green (40 ng/mL) and Dansyl-EDA-R6G (1 μg/mL). The cells were further incubated for 30 min and then analyzed with a confocal fluorescence microscope.

2.8. Ratiometric imaging of lysosomal acidity with Lyso-DR

For single lysosome acidity determination, 120 lysosomes were collected automatically and the data was analyzed with Imaris software. L929 cells and HeLa cells were respectively seeded on 35 mm glass-bottom dishes and incubated in DMEM medium for 24 h, followed by addition of Lyso-DR (1 μg/mL). The cells were further incubated for 30 min and then analyzed with a confocal fluorescence microscope. The ratio of the channel 1 (dansyl fluorescence@410–470 nm) to channel 2 (R6G-amide fluroescecne emission@565–625 nm) was calculated using the value of selected lysosomes given by the software. For average lysosomal acidity of cells, 5 cells were randomly selected where the pH of 120 lysosomes were determined and averaged.

2.9. Ratiometric imaging of lysosomal acidity in cells undergoing apoptosis and nercrosis

L929 cells were seeded on 35 mm glass-bottom dishes and incubated in DMEM medium for 24 h, then treated with 1 μM of staurosporine (STS) or 10 ng/mL of tumor necrosis factor-α (TNF) for 4 h to induce apoptosis and necrosis respectively. Cells were then incubated with Lyso-DR (1 μg/mL) for 30 min and then analyzed on a confocal microscope. A statistical analysis was performed with pH value of 20 treated or untreated cells.

2.10. Cell cytotoxicity assay

HeLa cells were seeded in 96-well plates at a density of 6×10^3 cells/well and incubated overnight in DMEM containing 10% fetal bovine serum (FBS). The cells were washed with PBS, and incubated in fresh medium containing different concentrations of Lyso-DR for various periods of time. The cells were incubated with medium supplemented with tetrazonium dye (MTT) (0.25 mg/mL) for 4 h at 37°C. The supernatant was removed and DMSO (100 μL) was added to dissolve the formazan. The plates were shaken for 5 min and then analyzed by SpectraMax M5 to record the absorbance (490 nm) of the wells.

3. Results and discussion

3.1. Characterization of Lyso-DR in buffers

Rhodamines are widely utilized in biological studies owing to their advantageous photophysical properties including high fluorescence intensity and photo-stability. Non-fluorescent rhodamine-lactams, featured by intra-molecular lactams, readily isomerize into highly fluorescent rhodamine-amides via pH mediated opening of the intramolecular lactams in living cells[15]. Although rhodamine lactams have been used to stain lysosomes in live cells, their applications in ratiometric pH sensing are limited[16]. In this report, conjugation of rhodamine 6G-lactam (R6G-lactam) with dansyl chloride via diethylenetriamine afforded Lyso-DR (Scheme 1), a ratiometric molecular pH-meter designed to selectively accumulate

in lysosomes in living cells *via* protonation of the amine-containing linker.

The ratiometric pH responses of Lyso-DR were characterized by fluorometry with dual wavelength excitation matching the dansyl/rhodamine fluorophores in buffers of various pH values (3.5–8.0). The fluorescence emission centered at 555 nm, characteristic to that of R6G, occurred at acidic media and intensified as buffer pH decreased, arising from in-situ formed R6G-amide via proton mediated opening of R6G-lactam (Scheme 1). The R6G-lactam was 800 fold more bright at pH 4.0 relative to that at pH 6.5 (Fig. 1A). In contrast to the dramatic increase of R6G-lactam fluorescence at acidic pH, the dansyl moiety exhibited decreased fluorescence emission (Fig. 1A). The reversed pH responses of dansyl/R6G-lactam diad enabled our proposed ratiometric imaging of lysosmal pH. The ratios of R6G-amide fluorescence intensity ($I_{555\ nm}$) to that of dansyl group ($I_{485\ nm}$) were plotted as a function of pH. Fig. 1B showed that subtle acidification in the range of pH 5.5–3.5 resulted in pronounced changes in the ratios. For instance, the *lg* ($I_{550\ nm}/I_{485\ nm}$) interval between pH 4 and pH 5 was 1 (Fig. 1B). In contrast, existing fluorescein based ratiometric sensors often exhibited moderate ratio changes (around 0.3) per pH unit [17–19]. The overlapping of the optimal pH sensing range of Lyso-DR (pH 6.0–3.5) with lysosome acidity window (pH 5.5–4.0) validated the utility of Lyso-DR as a molecular pH-meter for monitoring subtle acidic pH changes in living cells.

3.2. Lysosome-specific imaging for pH variations

3.2.1. Intracellular distribution of Lyso-DR.

With the sensitive ratiometric responses to acidic pH, Lyso-DR was evaluated for its capability to stain lysosomes in living cells. As shown in Fig. 2, confocal microscopic analysis of L929 cells co-stained with Lyso-DR and LysoTracker Green DND-26 (referred to as Lysotracker green) showed that R6G-amide and dansyl fluorescence, both present in cells, was super imposable with Lysotracker green, a lysosome-targetable dye. The colocalization revealed that Lyso-DR was exclusively confined in lysosomes where the non-fluorescent R6G-lactam was activated into fluorescent R6G-amide species (Scheme 1).

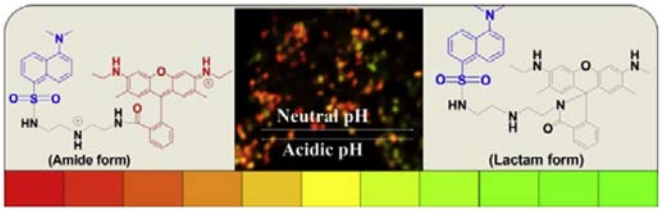

Scheme 1. Schematic diagram for the assay principle of the molecular pH-meter.

3.2.2. Comparison of acidotropic Lyso-DR to its structural analog

To demonstrate the structural factor that leads to accumulation of Lyso-DR in lysosomes, a new probe (Dansyl-EDA-R6G), where R6G-lactam was linked with dansyl moiety by ethylenendiamine, was synthesized and analyzed for its lysosome-targeting capability. As the structural analog of Lyso-DR, Dansyl-EDA-R6G differs from Lyso-DR in that its linker is immune to protonation in lysosomes (Fig. 3A). Fig. 3B and C showed that R6G-amide signals inside L929 cells colocalized with the fluorescence of Lysotracker green whereas the dansyl fluorescence was observed throughout the cells, suggesting that Danyl-EDA-R6G, distributed both intra- and extra-lysosomally, was regio-selectively activated in lysosomes to give R6G-amide. In contrast with the presence of extra lysosomal Danysl-EDA-R6G, the distribution of Lyso-RD within lysosomes highlighted the critical role of its diethylenetriamine linker which confers Lyso-DR the stringent selectivity to target lysosomes.

3.2.3. Assay with an ATP–H1 pump inhibitor

To further assess the pH dependent staining of lysosomes, L929 cells were incubated with Lyso-DR and BFA, which is an ATP–H1 pump inhibitor and is able to alkalinize the lysosomal pH [20], and then analyzed by confocal fluorescence microscopy to probe the effects of lysosomal pH on intracellular distribution of Lyso-DR. In sharp contrast with the punctate forms of Lyso-DR in control cells in Fig. 4, microscopic analysis revealed the pervasive distribution of Lyso-DR in cells treated with BFA, further proving lysosomal acidity mediated accumulation of Lyso-DR in living cells.

3.3. Imaging and quantitation of pH of individual lysosomes with Lyso-DR

To quantify lysosomal pH with Lyso-DR, a calibration experiment was first performed in HeLa cells which were first stained with Lyso-DR and then incubated in Briton buffer of various pHs supplemented with H^+/K^+ ionophore nigericin, a standard approach to homogenize intracellular pH to that of culture media [21]. The resultant cells were analyzed by confocal fluorescence microscopy for pH correlated dual emissions of Lyso-DR inside cells. Upon acidification of medium pH from 6.5 to 4.0, the dansyl fluorescence in cells slightly decreased whereas that of R6G channel increased. Fig. S1 shows the ratios of R6G-amide signals to dansyl fluorescence exhibited linear responses to pH changes in the range of pH 4.0–6.5.

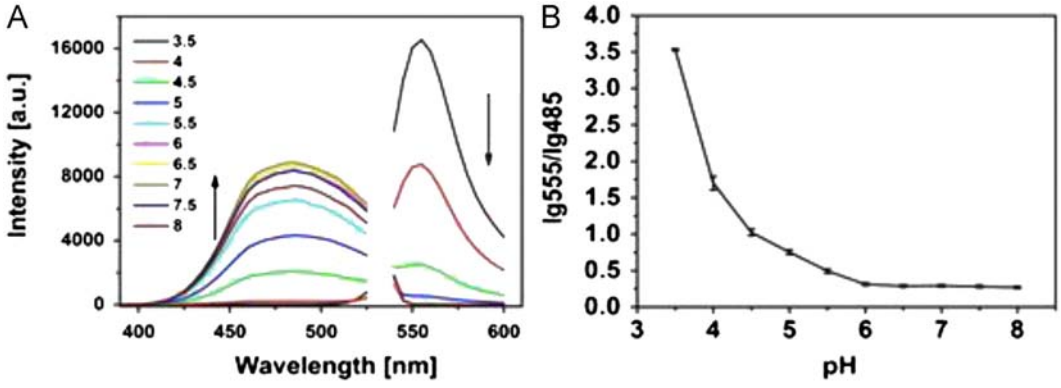

Fig. 1. pH dependent ratiometric fluorescence emission of Lyso-DR. (A) Fluorescence emission spectra of Lyso-DR (10 μg/mL) at pH 3.5–8.0 under dual-wavelength excitation (λ_{ex}@300 nm for dansyl group, 532 nm for R6G-lactam). (B) pH titration curves of *lg* ratios between fluorescence emission of R6G-amide (I_{555} nm) and that of dansyl group (I_{485} nm).

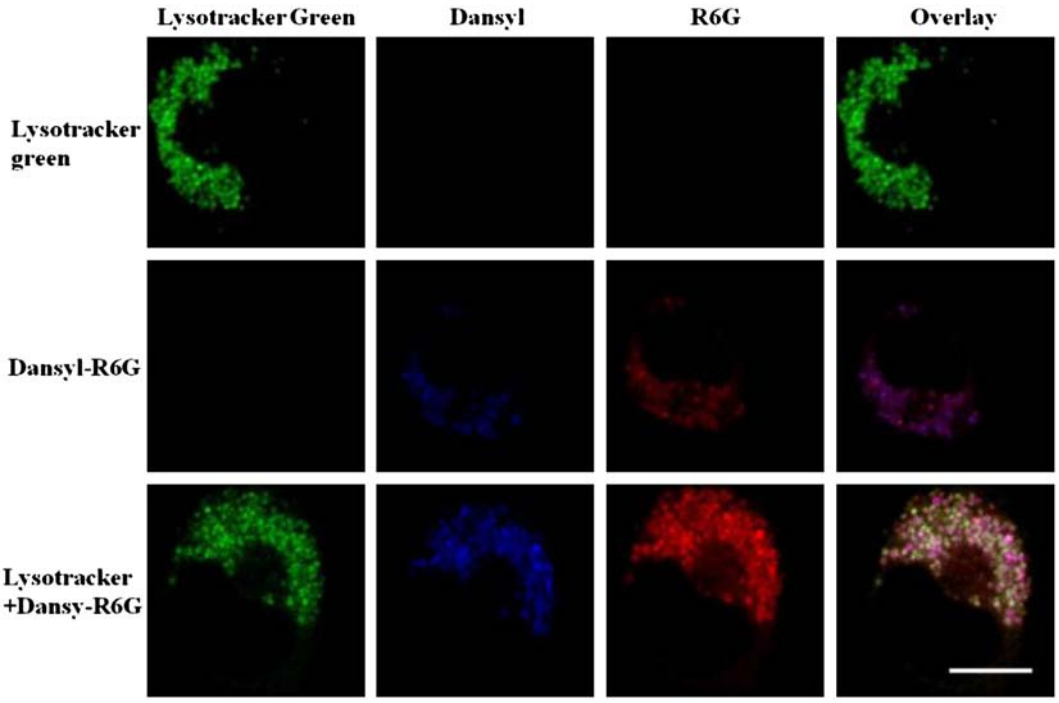

Fig. 2. Staining of lysosomes with Lyso-DR. L929 cells were respectively stained with Lyso-DR (1 μg/mL), Lysotracker green (0.4 μg/mL), or both. Intracelluar R6G-amide fluorescence was shown in red, dansyl fluorescence was shown in blue and that of Lysotracker green was marked in green. Bar, 10 μm. (For interpretation of the references to color in this figure legend, the reader is referred to the web version of this article.)

Demonstrated to be able to be responsive to changes on lysosomal pH in nigericin treated cells, Lyso-DR was further investigated for its capability to report lysosomal acidity in native HeLa and L929 cells. Confocal microscopy analysis of the cells pre-stained with Lyso-DR showed that dansyl fluorescence and R6G-amide signal were present in punctuate forms inside cells. Merging of both signals revealed colocalization where a variety of colors, ranging from green, orange to red, were observed in Fig. 5. The color variations, arising from varied ratios of dansyl fluorescence to R6G-amide fluorescence in individual lysosomes, were indicative of the lysosomal acidity. Hence, the microscopic images allowed convenient comparison of the relative acidity of individual lysosomes and their tempo-spatial distributions in living cells.

We further quantitate the lysosomal pH of HeLa and L929 cells with Lyso-DR by confocal fluorescence microscopy. With Lyso-DR, an individual lysosome resolution can be achieved (Fig. 6A). 120 lysosomes of a representative HeLa cell and a L929 cell were analyzed for the ratios of R6G-amide fluorescence to dansyl fluorescence based on the calibration curve shown in Fig. S1. The lysosomal acidity of 120 lysosomes was shown in Fig. 6B where the mean lysosomal pH of a HeLa cell is at about pH 4.5 while that of a L929 cell is at about pH 5.8 (Fig. 6B). Next, the mean lysosomal pH of 5 cells was determined using the same procedure and it was shown that the overall lysosomal acidity of HeLa cells is around pH 5.0 while that of L929 cells is at about pH 6.2 (Fig. 6C). *P* values calculated correspondingly were less than 0.05 that means the pH difference of these two kinds of cells was statistically significant. These data demonstrated the utility of Lyso-DR for the determination of the pH of individual lysosomes and the overall lysosomal pH in living cells.

3.4. Quantitation of lysosome pH of apoptotic cells and necrotic cells with Lyso-DR

Cell death often proceeds by ways of apoptosis, a degenerative and programmed process, or necrosis as the consequence of external injuries [22]. To explore the utility of Lyso-DR in reporting global changes of lysosomal pH in these cell death signaling events, L929 cells pre-stained with Lyso-DR were respectively cultured with STS or TNF-α [23,24].Stimulation of L929 cells with STS, an apoptosis inducer, rapidly induced decreasing of R6G signals, indicating alkalinization of lysosomal pH which is in agreement with the report that lysosomes were alkalinized in HL-60 cells during apoptosis [21]. Quantitative analysis of the average pH of 120 lysosomes from 10 cells showed that the lysosomal acidity of cells experiencing apoptosis was at about pH 6.2 while the cells undergoing necrosis are of similar pH to that of control cells (Fig. 7C). In contrast to the marked effects of STS on lysosomal pH, negligible alteration was observed on lysosomal acidity of L929 cells treated with TNF-α, suggesting that the lysosome pH remained largely unaffected during early necrosis process. Consistently, L929 cells undergoing necrosis induced by TNF-α is are featured by enhanced generation of oxygen radicals and cell membrane permeabilization whereas the structures of lysosomes remained largely intact [25].

3.5. Comparison of Lyso-DR with a commercial LysoSensor

Ratiometric measurement of lysosomal pH was reported to be achieved with commercial LysoSensors which are dual emissive dyes from Invitrogen. With the demonstrated capability to sense intralysosomal pH, Lyso-DR was further compared with commercial probes. Fig. S2 showed that Lyso-DR displayed competitive performance as that of LysoSensor Yellow/Blue. The cytotoxicity of Lyso-DR was evaluated in L929 cells by MTT assay as well. No detrimental effects on cell viability were observed at doses up to 100 μg/mL after incubation for 48 h (Fig. S3), suggesting that Lyso-DR is of low cell toxicity.

4. Conclusions

In summary, Lyso-DR, with pH activatable rhodamine-lactam bridged with dansyl fluorophore via an acidotrophic linker, was

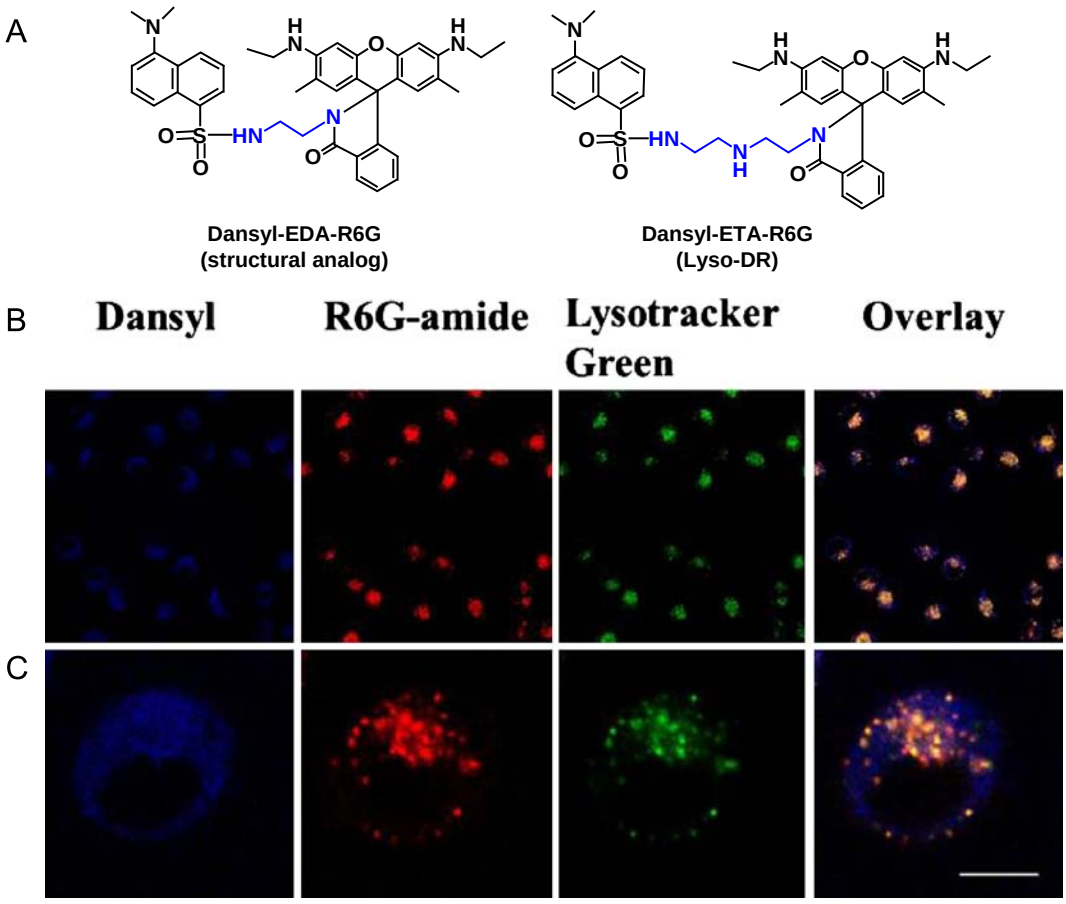

Fig. 3. (A) Structural difference between Lyso-DR and its analog Dansyl-EDA-R6G. Global view (B) and single cell image (C) of intracellular distributions of Dansyl-EDA-R6G as compared to Lysotracker green. L929 cells were cultured in DMEM medium spiked with Lysotracker green (40 ng/mL) and Dansyl-EDA-R6G (1 μg/mL), and then visualized with a confocal fluorescence microscope. The dansylfluorescecne (in blue) in 410–470 nm was collected using λ_{ex}@405 nm; R6G-amide fluorescence emisison@550–630 nm (shown in red) was collected using λ_{ex}@543 nm while Lysotracker green emissions@490–525 nm (shown in green) was recorded under λ_{ex}@488 nm. Overlay of R6G-amide signal with that of Lysotracker green was shown in yellow. Bar, 10 μm. (For interpretation of the references to color in this figure legend, the reader is referred to the web version of this article.)

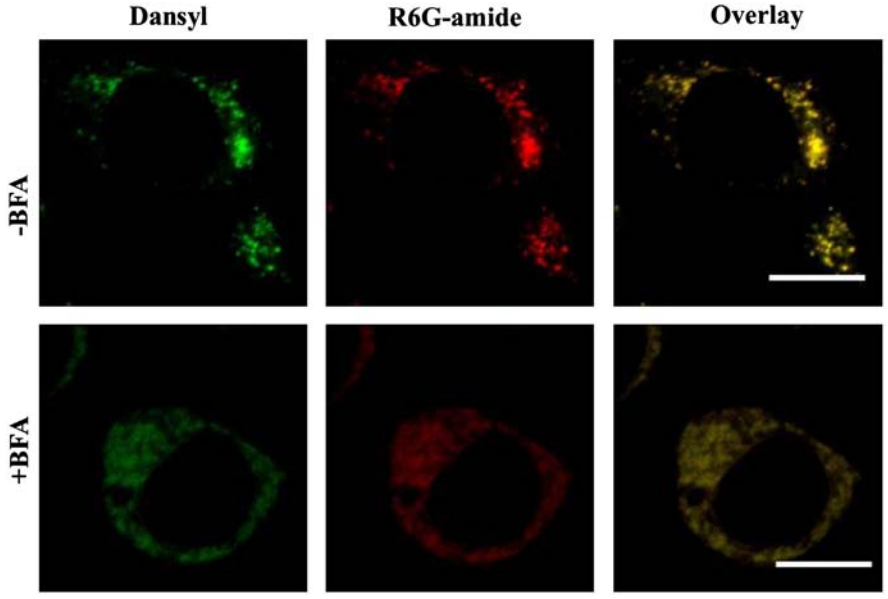

Fig. 4. Confocal microscopic images of pH dependent staining of lysosomes in a L929 cell treated with or without BFA. L929 cells, pre-incubated in DMEM medium spiked with or without BFA (100 nM) for 4 h, were further cultured in DMEM medium containing Lyso-DR (1 μg/mL) for 30 min and then analyzed with a confocal fluorescence microscope. Merge of R6G-amide (shown in red) and dansyl fluorescence (shown in green) was shown in yellow. Bar, 10 μm. (For interpretation of the references to color in this figure legend, the reader is referred to the web version of this article.)

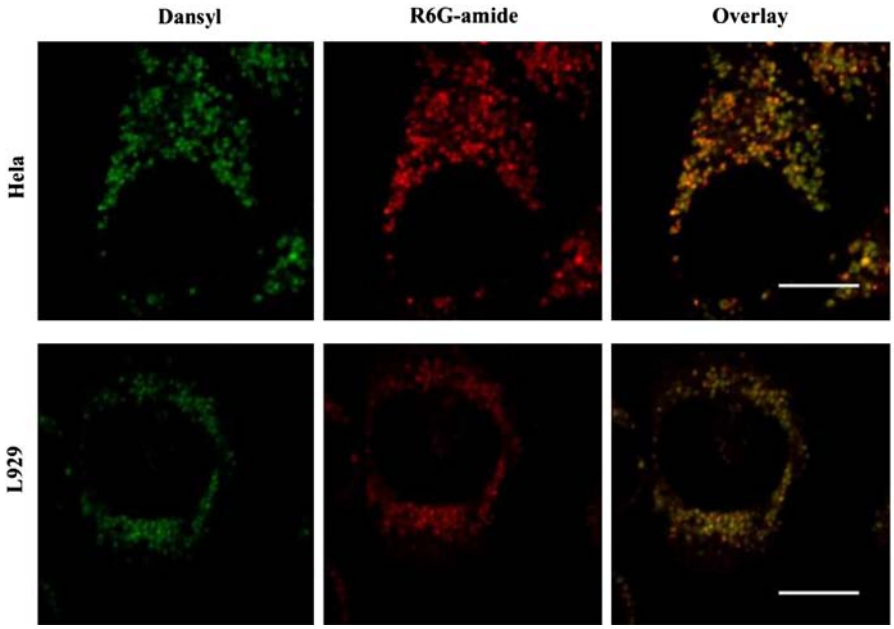

Fig. 5. Visualization of lysosomal pH in a HeLa cell and a L929 cell. L929 cells and HeLa cells were respectively incubated in DMEM medium supplemented Lyso-DR (1 μg/mL) for 30 min and then probed by confocal fluorescence microscopy. Dansyl fluorescence was shown in green and R6G-amide fluorescence was shown in red. Merging revealed colocalization of both signals where various colors ranging from pale green to red were observed. Bar, 10 μm. (For interpretation of the references to color in this figure legend, the reader is referred to the web version of this article.)

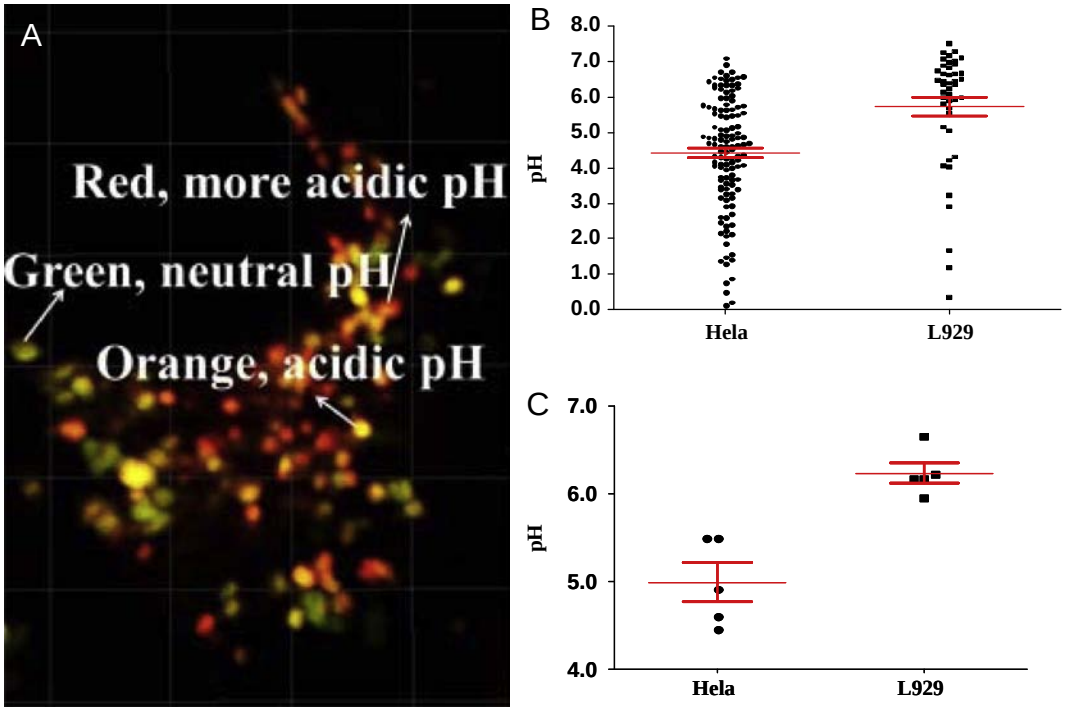

Fig. 6. Quantitation of lysosomal pH in in living cells with Lyso-DR. L929 cells and HeLa cells prestained with Lyso-DR (1 μg/mL) were visualized by confocal fluorescence microscopy. (A) Image of a HeLa cell stained with Lyso-DR. (B) pH values of 120 lysosomes in a HeLa cell or a L929 cell; the mean values were marked in red, $p < 0.001$. (C) lysosomal pH of five HeLa cells and five L929 cells, the lysosomal pH of each single cell was determined by the average lysosomal pH value of 120 randomLy selected lysosomes. Bar, 10 μm, $p < 0.05$. (For interpretation of the references to color in this figure legend, the reader is referred to the web version of this article.)

prepared for ratiometric sensing of lysosomal pH in living cells. The bioimaging can be performed by confocal fluorescence microscopy, allowing measuring lysosomal pH at an individual organelle level. Lyso-DR was proved to be highly efficiency in differentiating apoptosis vs necrosis cells. Compared with commercial lysosensors which often contain a single fluorophore, Lyso-DR consists of dansyl group and rhodamine moiety, two widely utilized fluorophores with distinguished photophysical properties. Design of molecular pH-meter via rational combinations of existing fluorophores in a way that could responds to specific analytes would be an attractive alternative to *de-novo* synthesis of new fluorophores for ratiometric imaging of analyte in living cells.

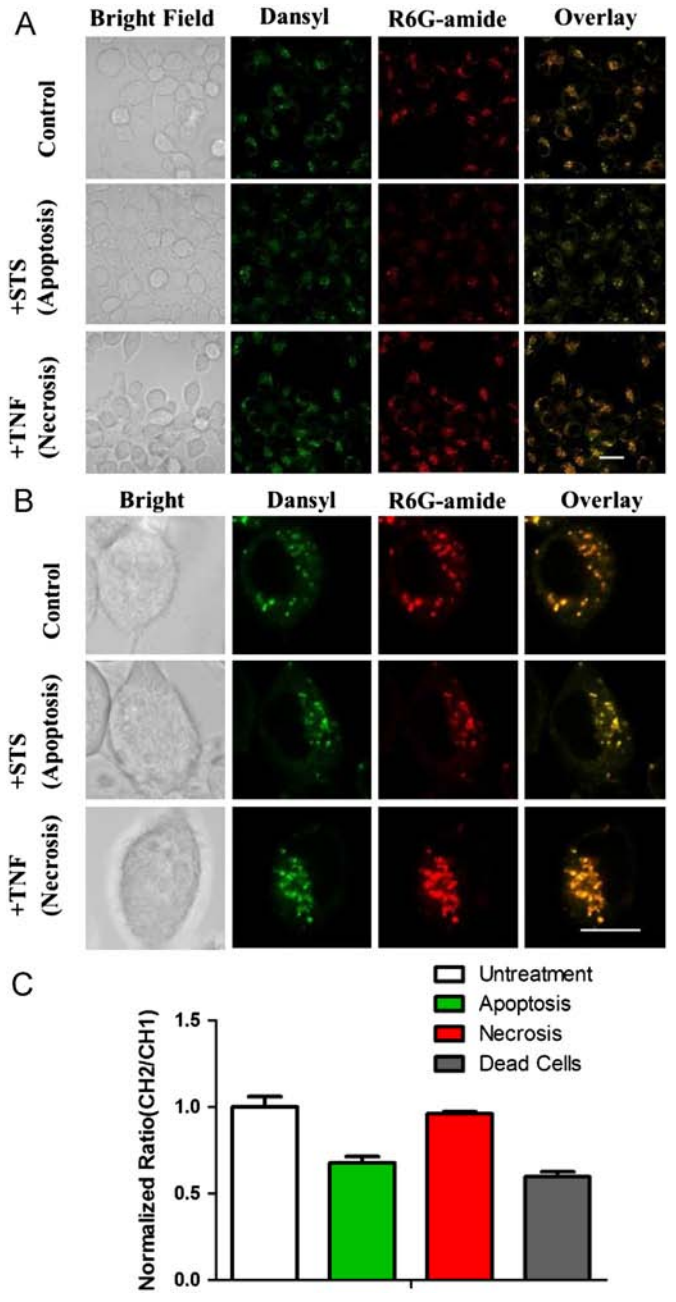

Fig. 7. Confocal fluorescence microscopic images of normal cells, apoptotic cells and necrotic cells. Dansyl fluorescence was shown in green and R6G-amide fluorescence was shown in red. Merging directly reflects the distinct acidity of corresponding cellular status. (A) broad view, (B) a single cell, (C) mean lysosomal acidity of 20 cells treated with STS (in green), TNF-α (in red) or no addition (in blank). Bar, 10 μm. (For interpretation of the references to color in this figure legend, the reader is referred to the web version of this article.)

Supporting information

Additional information as noted in text. This material is available free of charge via the Internet at http://www.sciencedirect.com.

Acknowledgments

Dr. S. Han was supported by grants from NSF China 21272196, 21072162, and the Fundamental Research Funds for the Central Universities 2011121020; Dr. J. Han was supported by grants from NSF China 31221065, 91029304, 81061160512 and 973 program 2009CB522200.

Appendix A. Supporting information

Supplementary data associated with this article can be found in the online version at http://dx.doi.org/10.1016/j.talanta.2013.05.036.

References

[1] E.S. Trombetta, M. Ebersold, W. Garrett, M. Pypaert, I. Mellman, Science 299 (2003) 1400–1403.
[2] Y. Urano, D. Asanuma, Y. Hama, Y. Koyama, T. Barrett, M. Kamiya, T. Nagano, T. Watanabe, A. Hasegawa, P.L. Choyke, H. Kobayashi, Nat. Med. 15 (2009) 104–109.
[3] H. Zerban, S. Radig, A. Kopp-Schneider, P. Bannasch, Carcinogenesis 15 (1994) 2467–2473.
[4] A.L. Edinger, C.B. Thompson, Curr. Opin. Cell Biol. 16 (2004) 663–669.
[5] A.C. Johansson, H. Appelqvist, C. Nilsson, K. Kågedal, K Roberg, K Öllinger, Apoptosis 15 (2010) 527–540.
[6] M.E. Guicciardi, M. Leist, G.J. Gores, Oncogene 23 (2004) 2881–2890.
[7] B. Turk, V. Turk, J. Biol. Chem. 284 (2009) 21783–21787.
[8] J. Han, K. Burgess, Chem. Rev. 110 (2010) 2709–2728.
[9] S. Charier, O. Ruel, J.B. Baudin, D. Alcor, J.F. Allemand, A. Meglio, L. Jullien, Angew. Chem. Int. Ed. (Engl.) 43 (2004) 4785–4788.
[10] J. Han, A. Loudet, R. Barhoumi, R.C. Burghardt, K. Burgess, J. Am. Chem. Soc. 131 (2009) 1642–1643.
[11] J. Llopis, J.M. McCaffery, A. Miyawaki, M.G. Farquhar, R.Y. Tsien, Proc. Natl. Acad. Sci. USA 95 (1998) 6803–6808.
[12] W. Shi, X. Li, H. Ma, Angew. Chem. Int. Ed. (Engl.) 51 (2012) 6432–6435.
[13] P.T. Snee, R.C. Somers, G. Nair, J.P. Zimmer, M.G. Bawendi, D.G. Nocera, J. Am. Chem. Soc. 128 (2006) 13320–13321.
[14] X. Zhou, F. Su, H. Lu, P. Senechal-Willis, Y. Tian, R.H. Johnson, D.R. Meldrum, Biomaterials 33 (2012) 171–180.
[15] H.N. Kim, M.H. Lee, H.J. Kim, J.S. Kim, J. Yoon, Chem. Soc. Rev. 37 (2008) 1465–1472.
[16] S. Wu, Z. Li, J. Han, S. Han, Chem. Commun. (Camb.) 47 (2011) 11276–11278.
[17] T. Jin, A. Sasaki, M. Kinjo, J. Miyazaki, Chem. Commun. (Camb.) 46 (2010) 2408–2410.
[18] J. Lei, L. Wang, J. Zhang, Chem. Commun. (Camb.) 46 (2010) 8445–8447.
[19] H.S. Peng, J.A. Stolwijk, L.N. Sun, J. Wegener, O.S. Wolfbeis, Angew. Chem. Int. Ed. (Engl.) 49 (2010) 4246–4249.
[20] T. Yoshimori, A. Yamamoto, Y. Moriyama, M. Futai, Y. Tashiro, J. Biol. Chem. 266 (1991) 17707–17712.
[21] C. Nilsson, K. Kagedal, U. Johansson, K. Ollinger, Methods Cell Sci. 25 (2003) 185–194.
[22] J. Searle, J.F. Kerr, C.J. Bishop, Pathol. Annu. 17 (2) (1982) 229–259.
[23] R. Bertrand, E. Solary, P. O'Connor, K.W. Kohn, Y. Pommier, Ex Cell Re 211 (1994) 314–321.
[24] P. Vandenabeele, W. Declercq, F. Van Herreweghe, T. VandenBerghe, Sc Signal. 3 (2010) re4.
[25] J. Grooten, V. Goossens, B. Vanhaesebroeck, W. Fiers, Cytokine 5 (1993) 546–555.